



## Full Review Article

## Shared mooring systems for offshore floating wind farms: A review

Hang Xu<sup>a</sup>, Shengjie Rui<sup>a,b,\*</sup>, Kanmin Shen<sup>a,c</sup>, Liangliang Jiang<sup>d</sup>, Haojie Zhang<sup>a</sup>, Long Teng<sup>a</sup><sup>a</sup> Zhejiang Key Laboratory of Offshore Geotechnics and Material, College of Civil Engineering and Architecture, Zhejiang University, Hangzhou, 310058, China<sup>b</sup> Norwegian Geotechnical Institute, Sandakerveien 140, Oslo, 0484, Norway<sup>c</sup> PowerChina Huadong Engineering Corporation Limited, Hangzhou, 311122, China<sup>d</sup> Department of Chemical and Petroleum Engineering, The University of Calgary, Calgary, Alberta, Canada

## ARTICLE INFO

## Keywords:

Floating offshore wind turbines  
Wind farm  
Shared mooring  
Shared anchor  
Renewable energy

## ABSTRACT

Offshore wind energy, as a form of renewable power, has seen rapid development in recent years. While fixed-bottom wind turbines are typically used in water depths less than 50 m, the utilization of floating offshore wind turbines (FOWTs) becomes essential for deeper waters. Secure and effective mooring systems play a crucial role in making FOWTs commercially viable. The concept of a shared mooring system offers an innovative solution for deploying floating wind farms in clusters or arrays, which can reduce overall construction costs for large-scale floating wind farms. It is imperative to optimize the shared mooring arrangement for maximum cost-effectiveness and wind farm stability. However, implementing a shared mooring system introduces complexity to the dynamics of FOWTs, requiring the development of advanced simulation tools to meet modelling requirements. Under the shared mooring arrangement, mooring lines and anchors face more significant challenges, such as chain-seabed interactions, soil cyclic weakening, and anchor out-of-plane loading, which underscore the need for innovative, reliable, and efficient shared anchor designs. This article offers an overview of the current research status on shared mooring systems for floating wind farms, which might serve as a valuable reference for the construction of large-scale floating wind farms worldwide.

## 1. Introduction

A rising energy demand and mounting environmental challenges render traditional fossil fuel sources facing increasing limitations in meeting sustainability requirements [1,2]. Renewable energies, e.g., solar energy [3], wind energy [4], hydrogen [5], and geothermal energy [6], have received widespread attention. Over recent years, offshore wind power has gained prominence in the global renewable energy market due to its abundant reserves, minimal environmental impact, renewable nature, and enhanced stability [7–9]. Statistics reveal a significant surge in the global offshore wind power sector over the past decade, with an average annual growth rate of 36%. The cumulative installed capacity has now reached 56 GW, with annual new installations growing from 1 GW in 2011 to 21.1 GW in 2021, a twentyfold increase [10]. The outlook for offshore wind power in the medium to long term remains highly optimistic [11]. Projections from BNEF and 4C Offshore [12] suggest that by 2031, the cumulative global offshore wind power capacity could reach 260–290 GW, exceeding the current total capacity by more than fivefold.

Compared to nearshore areas, deep offshore regions (with water depths exceeding 50 m and located more than 50 km offshore) offer more stable wind speeds and abundant wind energy resources (see Fig. 1a and b). Additionally, these areas are far remote from human habitats, minimizing human activity impact and reducing potential conflicts associated with nearshore utilization. Consequently, the development of deep offshore wind energy presents the predominant trend in offshore wind power. Floating offshore wind turbines (FOWTs) have emerged as the logical choice, considering current technological and economic assessments. According to DNV [13], it is projected that by 2050, the installed capacity of floating offshore wind power will reach 250 GW, representing over 20% of the offshore wind power market and contributing approximately 2% to global electricity supply. Currently, four commercial floating offshore wind farm projects are operational worldwide, namely, Hywind Scotland, WindFloat Atlantic, Hibiki Floating Offshore Wind Farm, and Kincardine Offshore Wind Farm (see Fig. 2a–d). However, it is essential to acknowledge that the overall development of global floating offshore wind farms is still in its early stages and has not yet achieved widespread commercial viability, primarily due to the challenge of cost

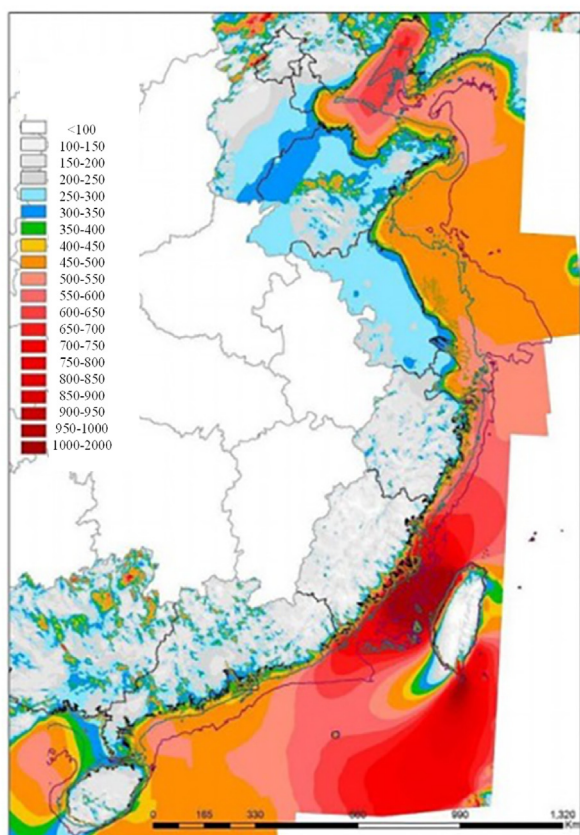
\* Corresponding author. Zhejiang Key Laboratory of Offshore Geotechnics and Material, College of Civil Engineering and Architecture, Zhejiang University, Hangzhou, 310058, China.

E-mail address: [shengjie.rui@ngi.no](mailto:shengjie.rui@ngi.no) (S. Rui).

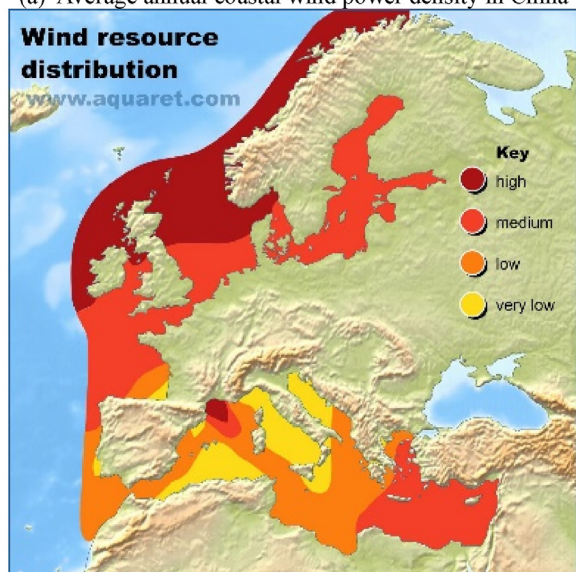
<https://doi.org/10.1016/j.enrev.2023.100063>

Received 18 October 2023; Received in revised form 1 December 2023; Accepted 3 December 2023

2772-9702/© 2023 The Authors. Published by Elsevier Ltd on behalf of Shenzhen City Clean Energy Research Institute, Shenzhen University. This is an open access article under the CC BY-NC-ND license (<http://creativecommons.org/licenses/by-nc-nd/4.0/>).



(a) Average annual coastal wind power density in China



(b) Wind resources distribution in Europe (www.aquaret.com)

Fig. 1. Distribution of coastal wind energy.

control.

Based on existing reports and data, it is evident that foundation costs for FOWTs can represent up to 30% of the total cost [14,15]. For FOWTs, the cost allocation for mooring systems, including winches, cable handlers, mooring lines, anchors, clump weights, and buoyancy, is expected to be even higher, potentially surpassing the cost of the wind turbine equipment itself [16]. As the scale of commercial FOWTs increases to hundreds of units, it is anticipated that manufacturing and installation costs for the mooring system will become considerably more expensive. This presents a pressing challenge that requires attention in the field of

floating offshore wind power.

Recently, the introduction of shared mooring design has presented a novel solution for deploying clustered or arrayed floating offshore wind farms. This concept departs from the conventional 'one anchor to one line' approach by connecting different FOWTs or anchors. This innovation significantly reduces mooring system construction, transportation, installation costs, and associated seabed geotechnical survey expenses. It holds substantial potential for advancement in the floating offshore wind power sector. However, as a relatively new mooring method, the shared mooring approach is currently in the conceptual design stage and lacks specific design standards. In contrast to single FOWTs, the shared mooring approach treats the entire wind farm as a unified entity, introducing more complex challenges, including turbine dynamics, mooring system coupling effects, and anchor load design. In-depth research and comprehensive evaluations are crucial to properly assess the feasibility of this approach.

This article offers an overview of the current research status on shared mooring systems for floating wind farms, covering layout forms of shared mooring wind farms, methods for analysing the dynamic behaviour of shared mooring FOWTs, characteristics of load transmission in shared mooring lines, and the load-bearing properties of shared anchors. This paper can serve as a reference for future floating wind farm construction worldwide.

## 2. Overview of floating wind farm

Floating wind farms are a type of offshore wind power generation system that uses an array of wind turbines on floating platforms instead of fixed foundations rooted to the seabed [17]. In addition to the turbine, an individual FOWT primarily comprises three major marine components: a floating platform, mooring lines, and mooring anchors.

### 2.1. Floating platforms

The designs of floating wind turbine platforms, including their associated components (moorings, anchors), are mainly derived from the technologies used in the oil and gas industries. Typologies of floating platforms for offshore wind currently can be divided into four general categories, namely Barge, Semi-submersible, SPAR and Tension Leg Platform (TLP), as shown in Fig. 3a. The different types of platforms are characterized by their hydrostatic stabilities and mooring system features [18–20], and Fig. 3b shows principal stabilized methods of these types of floating support platforms described above. In practice, all floating concepts are actually hybrid designs that gain static stability from all three methods, although generally relying on one primary source for stability [21].

### 2.2. Mooring lines

Each floating platform is tethered to the seabed with mooring lines that prevent it from drifting off and transfer the loads from the marine environment to the mooring anchors. From the geometric configurations, the mooring system includes two main categories: catenary mooring and (semi) taut mooring [23,24], as shown in Fig. 4. Catenary moorings are generally utilized in shallow water, and the restoring forces are mainly provided by the mooring line gravity [25]. Therefore, chain is usually used for catenary mooring for increasing the stiffness of mooring line and reducing the lying length to improve mooring performance and reduce the costs. And taut mooring is generally applicable to deep water [26]. Taut moorings usually adopt mooring lines with lightweight, such as steel wires or synthetic fiber ropes to resist vertical loads, which bring challenges to anchor design, especially in deep sea especially for TLP.

From the fairlead connections, the mooring systems include multi-point and single-point moorings. A multi-point mooring is to distribute mooring lines from different attached points (fairleads) and is main mooring form used in FOWTs. In the case of a FOWT, employing a multi-

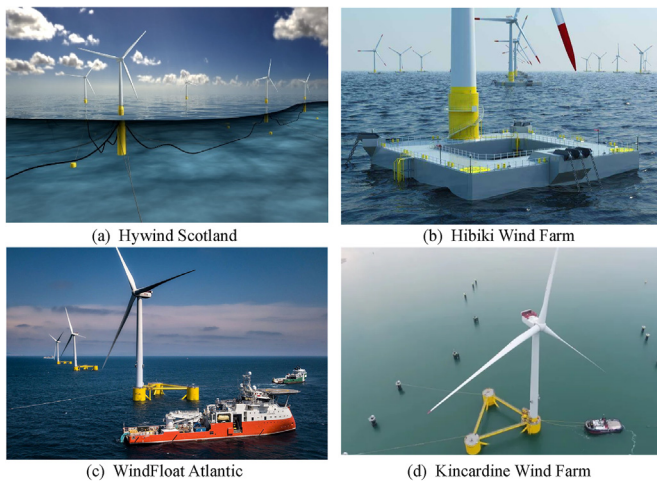


Fig. 2. Commercial floating wind farm.

point mooring system can distribute the force points, thereby enhancing the stability of the structure. Furthermore, it allows for alleviating potential weaknesses associated with relying solely on a single point. However, it should be noted that this approach introduces an unavoidable redundancy in the mooring design, which may lead to inefficiencies and wastefulness [27].

### 2.3. Mooring anchors

Anchors provide the final resistances to fix the floating structures. Different anchors are adopted based on the force characteristics transferred from the mooring line, design requirements and soil properties, which will be further discussed in Sections 5 and 6. Nowadays, the principal anchors employed in floating wind farms include suction anchor, pile anchor, plate anchor and gravity anchor, and their installations and capacities are two main aspects. Due to the complex load conditions in which the FOWTs operate, several novel anchors are currently being developed, such as suction embedded plate anchor (SEPLA), dynamically installed anchors (DIAs), screw anchors, etc [28–30]. Ultimately, anchor choice will be project and site-specific, often dictated by the seabed conditions.

## 3. Shared mooring wind farm layout and optimization method

### 3.1. Relationship between layout and economy

A shared mooring system is a novel design aimed at reducing mooring system costs for a floating wind farm, which can be implemented through two fundamental forms: shared anchors and shared lines, or a combination of both, as depicted in Fig. 5.

Fontana et al. [31] first introduced the concept of “Multiple-Line Anchor System”, which involves connecting mooring lines from different FOWTs to a shared anchor, thereby reducing the number of required anchors. For shared mooring floating wind farms with a symmetric geometrical structure, Fontana et al. [31] defined the relationship for mooring efficiency. Disregarding the edges that are not part of the shared anchor, the relationship can be expressed as follows:

$$n_A = n_T \frac{n_{AT}}{n_{TA}} \quad (1)$$

where  $n_{AT}$  represents the number of anchors connected to each FOWT, generally  $n_{AT} \geq 3$ .  $n_{TA}$  represents the number of FOWTs connected to each anchor,  $n_T$  is the total number of FOWTs in the wind farm, and  $n_A$  is the number of anchors required for the wind farm. Taking a typical

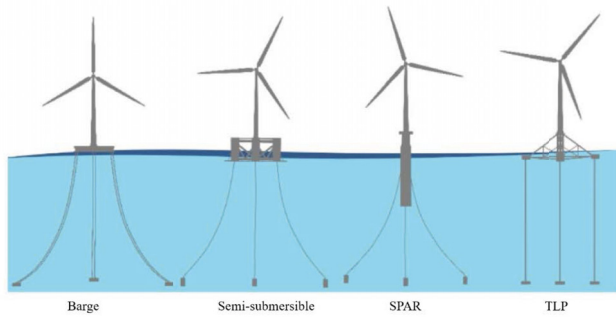
symmetric 3-line shared mooring system as an example, when the wind farm is sufficiently large and edge effects are neglected,  $n_A$  is equal to  $n_T$ , meaning that the number of FOWTs and the required number of anchors are the same. From the equation, it can also be observed that  $n_{TA}$  is inversely proportional to  $n_A$ , indicating that a larger multi-line shared anchor design leads to a more significant optimization of anchor numbers [32], as shown in Fig. 6. Fontana et al. [31] further noted that while the use of multi-line anchors may reduce the number of anchors required for the wind farm, it may necessitate changes in anchor size, type, and installation method. Nevertheless, the number of anchors remains a decisive criterion for evaluating the mooring efficiency and economic viability of the wind farm.

In addition to shared anchors, adjacent FOWTs can also share mooring lines, thereby further reducing the number and length of required cables [33,34]. Although the implementation of shared mooring lines in floating offshore wind farms has not been realized yet, the concept has been explored in early-stage arrayed wave energy converter (WEC) projects [35]. Goldschmidt & Muskulus [33] investigated the dynamic properties and the cost-saving potential of shared mooring systems for a row, triangular, and rectangular arrangement of FOWTs in the frequency domain, and found that significant cost reductions of up to 60% in mooring systems and 8% in total system costs could be achieved. Hall et al. [36] made a comprehensive comparison between the total array station-keeping costs for a ten-turbine floating wind farm utilizing shared mooring lines and shared anchors, and a conventional design using three or four separate mooring lines. The results showed a relative reduction in mooring system installation costs of 26% and 34% for the shared mooring line and shared anchor designs, respectively. Overall, the economic benefits of both shared mooring anchors and shared mooring lines are evident.

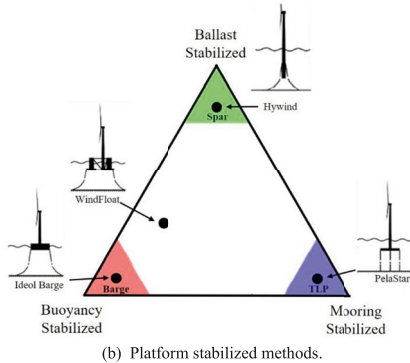
### 3.2. Layout optimization method

To further reduce the number of mooring lines or anchors in floating wind farms, different layouts of shared mooring systems have been proposed and compared in search of the optimal arrangement. Connolly & Hall [37] proposed an initial dimensioning design algorithm for a shared mooring system suitable for small-scale floating offshore wind farms. They designed and analyzed a floating offshore wind farm consisting of four wind turbines, considering three alternative shared mooring layouts and four water depth environments. Factors such as platform displacement, mooring line tension, and construction costs were compared under different conditions. The findings indicate that with the appropriate design of shared mooring layouts, platform displacement, and mooring line tension can be maintained at lower levels. Additionally, significant cost reduction is achieved when water depths exceed 400 m.

Based on a linearized model of the mooring line force-displacement response, Wilson et al. [38] proposed a rapid and optimal layout design method for the mooring lines in an array-based floating offshore wind farm. They compared the restoring force contribution of mooring lines in regular and irregular layouts. The results reveal that a regular polygon layout generates uniform restoring characteristics for all wind turbines, resulting in collective array displacement. In this case, shared mooring lines are solely used to maintain mooring line tension, and their contribution to the restoring force can be neglected. In addition, for irregular layout configurations, the optimal mooring system becomes more complex and places higher demands on the restoring capabilities of shared mooring lines. Devin et al. [39] combined multivariate genetic algorithms with Bayesian optimization to conduct predictive analysis and reliability optimization of construction costs, mooring system failure rates, and maintenance costs in extreme operating conditions for shared-array floating offshore wind farms. The results indicate that the reliability of the shared mooring system is highly sensitive to variations in wind turbine costs and downtime. This finding highlights the importance of further research on the failure modes of FOWTs. Hallowell et al. [40] conducted 100,000 simulations of Monte-Carlo simulations on



(a) Four main types of floating platforms (Reproduced under the terms of the CC-BY license. [22] Copyright 2022, MDPI).



(b) Platform stabilized methods.

Fig. 3. Typologies of floating platforms [22].

FOWTs with single-line anchor system only and FOWTs with 3-line anchor system, and indicated that progressive failures were a contributing factor in the decrease in multilane system reliabilities when compared to the single-line system, and should be taken into account in the design of multilane FOWT systems. Hallowell et al. [41] also proposed that modest (10%) increases in the design anchor capacity in a 3-line wind farm can completely mitigate the risk of cascading or progressive failure of the interconnected anchor system and restore reliability equivalent to that in a wind farm using single line anchors. Yamamoto & Colburn [42] discussed the layout of shared mooring lines and shared anchors, suggesting that wind farms are generally configured in triangular or hexagonal shapes. However, further practical evidence is required to support this. It is worth noting that in currently commercially operational floating wind farm projects, the predominant approach involves each FOWT being equipped with three mooring lines and three anchors [43]. Therefore, future development may focus on the design optimization of shared anchor systems based on the configuration of a single wind turbine with a three-line mooring arrangement.

#### 4. Dynamic analysis method for shared mooring wind farm

##### 4.1. Numerical methods

Considering that shared mooring floating offshore wind farms are still in the conceptual design stage, numerical simulations are currently the primary method for optimizing the design and conducting dynamic analysis of shared mooring systems. Compared to onshore or fixed-bottom offshore wind turbines, FOWTs experience larger loads and displacements under the combined effects of wind and waves [44]. The operating environment of deep-water FOWTs is highly variable, with a complex system configuration and prominent coupled dynamic issues [45]. The complexity of the coupled dynamic issues in shared mooring FOWTs arises from the coupling between the upper wind turbine and the lower floating foundation on each FOWT, as well as the significant coupling effects between different FOWTs. This necessitates the inclusion of the entire wind farm in a unified analysis framework when conducting

numerical simulations of FOWTs, taking into account the coupling effects between different modules such as aerodynamics, servosystems, elasticity, hydrodynamics, and mooring systems. This can be achieved by further developing or expanding upon existing commercial or open-source software based on some fundamental theories and principles.

For example, the aerodynamic modelling of wind turbines often employs the blade element momentum (BEM) theory, which has been proven to be highly applicable in practice [46]. Similarly, the hydrodynamic loads on floating platforms are typically modelled using well-established methods previously used in the oil and gas industry, such as potential flow theory and the Morison equation. For the analysis of the overall dynamic response of FOWTs, methods such as multibody dynamics or finite element analysis are commonly employed [47]. Currently, there are three main categories of integrated analysis software for individual FOWTs (see Table 1) [48]: 1) commercial software represented by Bladed and HAWC2; 2) open-source software represented by FAST/OpenFAST; 3) combined computational software developed by universities or research institutions that integrate commercial and open-source tools, such as SIMA, CHARM3D-FAST. It is worth noting that some traditional floating structure analysis software, such as OrcaFlex, have also developed simulation modules specifically for floating wind turbines in their latest versions [49].

Prevailing methods for an individual FOWT provide the support technology for the dynamic analysis of shared mooring wind farm while some special key points should be cared. First of all, the most important is the definition of shared mooring lines between interconnected FOWTs. In other words, an approach is required to define the coupled response of both FOWTs from shared mooring lines [50]. For a simplified analysis, it can be easily achieved by defining the catenary shape of the line and the relative FOWT positions under the Quasi-static model [38,51]. For dynamic analysis, nevertheless, it is more complicated that the mooring tension is fully coupled with platform motions, which implies that the displacements between different FOWTs must be exchanged in time after completing the dynamic analysis of each individual FOWT. Zhang & Liu [52] employ the coupling between FAST and AQWA to establish a reliable framework for data transfer through transformation of reference coordinate systems between different structures. Lozon & Hall [50] developed an open-source method by creating input and output meshes and converting local and global motions to overcome the limitations in OpenFAST and FAST. farm and consider the impacts of shared moorings on line tensions, platform motions, tower and anchor loads, and failure scenarios. However, few research on this aspect is available currently. Existing research on shared mooring line dynamics mostly used proprietary simulation tools like Ocaflex, and HAWC2 as mentioned before, and focused on smaller arrays of two to four turbines.

In addition, it is also significant to consider the potential coupling effects between different FOWTs in terms of aerodynamics and hydrodynamics. For example, there is a noticeable “aerodynamic wake effect” present among different wind turbines in the wind farm. The wake effect refers to the phenomenon where a wind turbine extracts energy from the wind, resulting in a downstream region of reduced wind velocity, known as the wake zone [53]. This uneven distribution of wind speeds in the wind farm can affect the operational performance of each wind turbine, subsequently impacting the overall operation and power output of the wind farm [54]. The wake effect is influenced by various factors, including the size of the wind farm, rotor diameter, thrust coefficient, wind speed, and wind direction [55]. This effect can be mitigated by increasing the distance between different FOWTs [56]. However, this approach also requires larger wind farm sizes and longer mooring line lengths, posing significant challenges in terms of construction costs. Additionally, having adjacent floating platforms situated too closely together can induce vortices and turbulence, altering the wave energy field and potentially affecting platform stability. These factors should be taken into consideration as well.

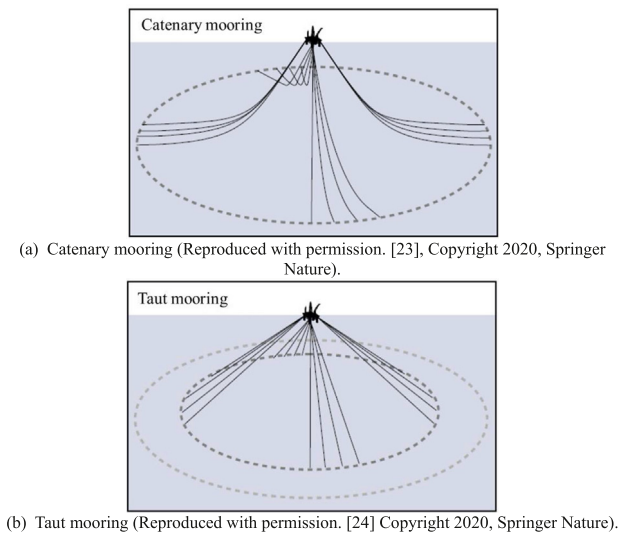


Fig. 4. Two main mooring categories.

#### 4.2. Dynamic influence

In general, there is currently a relatively limited amount of literature available on the simulation of floating offshore wind farms, as well as a lack of established design standards and unified simulation tools or methods. As a complex system, FOWTs simultaneously under aerodynamic loads on the wind turbine (both rotor and tower) and hydrodynamic loads on the floating platform, and these loads will interact with the motion and the deformation (wind turbine only) of the FOWT, which is one of the major concerns in the analysis of the responses of FOWTs [52]. For the turbine-related loading analysis above the tower base flange, these concerns mainly focus on the evaluation of bending moments, shear force amplitudes, or fatigue damage at the tower top, tower base, and blade roots under extreme conditions (like typhoon scenarios), and the reinforcement design of local structures and intelligent control of wind turbines with numerous studies been conducted [57–59]. As for the shared mooring system, the current research primarily emphasizes the dynamic response of the floating foundation below the tower base, as well as the mooring tension of the shared lines.

The existing numerical simulations are often based on fundamental theoretical assumptions and simplified layout configurations. Hall & Connolly [60] conducted response simulations of a square-shaped floating offshore wind farm with four FOWTs utilizing the coupling between FAST V7, MoorDyn, and a program for precomputed wave kinematics and loading for the entire wind farm considering irregular waves

and turbulent wind conditions. It is important to note that the simulations by Hall & Connolly [60] primarily focused on the structural coupling of the mooring system and the FOWTs, without including the wake effect.

Gözcü et al. [34] extended the commercial software HAWC2 to HAWC2. Farm and simulated the operation of two IEA 15 MW SPAR-type FOWTs under shared mooring lines and shared anchors based on the actual conditions of the two sites. The results showed that by adjusting the length of the mooring lines, the shared mooring system could achieve a similar natural frequency as a single mooring system. However, compared to a single mooring system, the shared mooring system exhibited higher mooring line tensions and platform displacements. Pillai et al. [61] employed the latest version of the Orcaflex software to perform coupled modeling of a semi-submersible floating wind farm, based on the IEA 15 MW design. Ding et al. [62] conducted simplified numerical simulations of the hydrodynamic performance of a square  $3 \times 3$  SPAR-type floating wind farm using the commercial software AQWA by ignoring the rotational movement of the blades. It was discovered that the proposed floating wind farm exhibits reduced sway response compared to a single FOWT under both extreme and normal operating conditions, with the degree of change being less significant as the severity of the operating conditions increases. Similarly, Yue et al. [63] established an array-type offshore wind farm using the AQWA software for a semi-submersible platform. They employed the DLL (dynamic link library) to calculate the aerodynamic loads. The results revealed that the array semi-submersible floating wind farm not only exhibits reduced sway amplitude but also demonstrates remarkable resistance to yaw and roll. Additionally, it shows enhanced stability in terms of nacelle vibration. However, the stability in heave and pitch is comparable to that of a single FOWT condition.

Moreover, He et al. [64] analyzed the frequency response characteristics of the Barge type platform for the second-order array floating wind farm under varying wind and wave directions. The results indicated that the sway and roll responses of each platform increased with the incident wave angle, while the pitch response decreased. The heave and surge responses were practically unaffected by the direction of wave incidence. Zhang & Liu [52] proposed a coupling analysis framework for FOWTs considering the interaction between aerodynamic and mooring forces at the tower base using the FAST and AQWA software. It was found that the anisotropic stiffness and the displacement of FOWTs are determined by aerodynamic loads. Meanwhile, the tension in mooring lines is influenced by both wind loads and wave loads. Further analysis of mooring line failure in the shared mooring system indicated that the tension response in mooring lines is highly sensitive to mooring failure and subsequent progressive failure. Munir et al. [65] conducted a study on two semi-submersible FOWTs with shared anchor lines using SIMA, considering the impact of different distances between platforms. The results revealed that shared mooring lines magnified the maximum surge

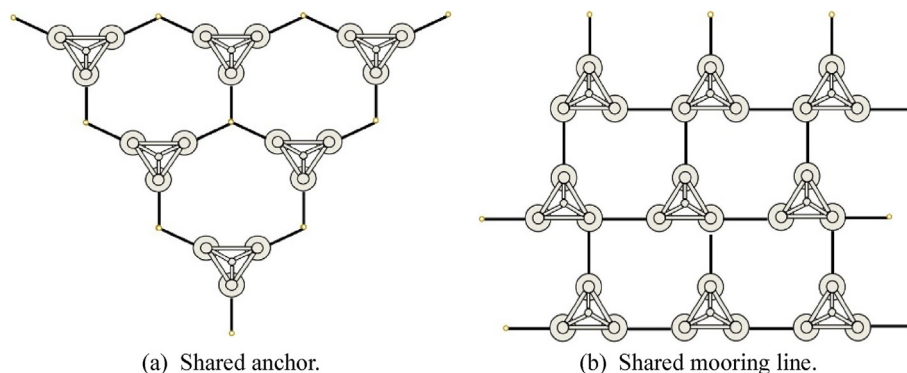
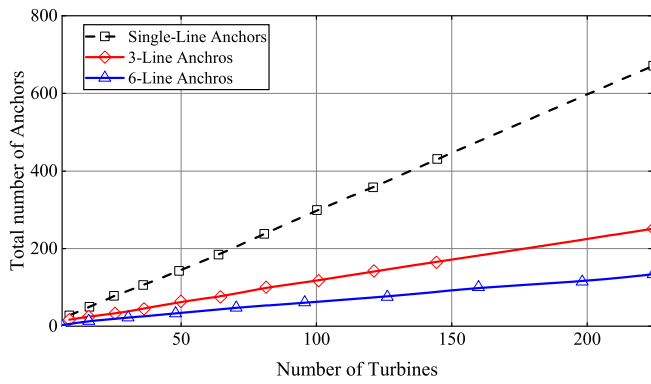
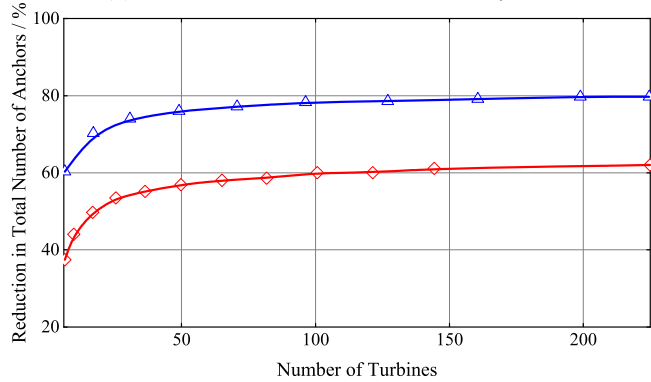


Fig. 5. Implementation form of shared mooring system.



(a) Anchor numbers of different layout.



(b) Reduction of anchor numbers in different layout.

Fig. 6. Calculation of anchors corresponding to different multi-line anchor layouts (Adapted with permission [32]. Copyright 2018, Wiley).

and sway motions, as the mooring restoring stiffness decreased. The spacing between platforms had no significant impact on the motions, indicating that the contribution of shared anchor mooring to platform restoring characteristics is minimal.

It should be noted that different software or models have varying capabilities due to their underlying theories. Currently, the most advanced simulation tool for floating offshore wind farms is FAST. Farm, developed by the National Renewable Energy Laboratory (NREL). FAST. Farm uses OpenFAST to solve the aero-hydro-servo-elastic dynamics of each turbine, but considers additional physics for wind farm-wide ambient wind in the atmospheric boundary layer; a wind-farm super controller; and wake deficits, advection, deflection, meandering, and merging [66], as shown in Fig. 7. The open-source nature of FAST. Farm allows easy accessibility to its example models online, greatly facilitating the modeling work for floating offshore wind farms and contributing to

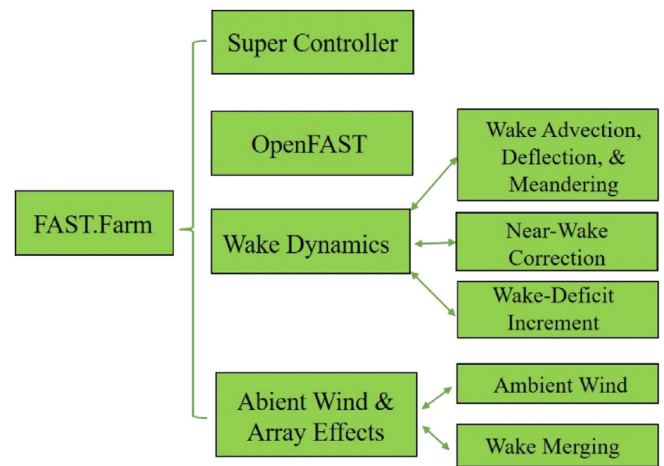


Fig. 7. Modules of FAST. farm.

its widespread adoption.

## 5. Load transfer characteristics of shared mooring system

### 5.1. Load calculation method of shared mooring line

For shared mooring system, the mooring line tension is typically calculated using two methods: static analysis [67], and dynamic analysis. The dynamic analysis methods, e.g., the lumped mass approach represented by MoorDyn, is widely used and takes into account the combined effects of gravity, hydrodynamic forces, and elastic forces [68]. The latest mooring module, MoorDyn V2 [69], integrated into OpenFast, further extends the linear elastic model and develops the methods for dynamically simulating mooring line failures.

It is worth noting that due to the lack of consideration for the geological properties of the seafloor, nearly all commercially available hydrodynamic analysis software lacks the modelling of the soil-embedded section of the mooring lines, as illustrated in Fig. 8. However, the line-seabed interaction influences the load magnitude and direction acting on the anchor padeye, which changes its failure mode [70]. Furthermore, the interaction between the mooring lines and the seabed is influenced by the soil properties and types, e.g., sandy or clayey seabeds. In the case of a clayey seabed, the clay rate effect, strain softening, and cyclic degradation are basic properties, which are partly considered in some studies [71–75] and need to be comprehensive considered [76]. As for sandy seabed, though some interesting tests have been conducted in cyclic chain-sand interaction [77,78], 3D chain-sand dynamic interaction is still unrevealed, which limits the analysis of the load direction on the anchors in sand.

Table 1  
Single FOWT integrated analysis software.

| Codes                | Developer | Availability   | Aerodyn   | Hydrodyn                                 | Elastodyn                        | Servodyn         | Mooring                                 |
|----------------------|-----------|----------------|---|--|----------------------------------|------------------|---|
| Bladed               | DNV-GL    | Commercial use | BEM/Generalized dynamic wake model + Dynamic inflow + Dynamic stall | Potential flow theory + Morison equation | MBS <sup>1</sup>                 | DLL <sup>4</sup> | FEM                                     |
| HAWC2                | DTU       | Commercial use |   | Morison equation                         | MBS/FEM <sup>2</sup>             | DLL + Simulink   | FEM                                     |
| FAST/ OpenFAST       | NREL      | Open source    |   | Potential flow theory + Morison equation | FEM + (Modal <sup>3</sup> / MBS) | DLL + Simulink   | QSCE <sup>5</sup> +LM <sup>6</sup> +FEM |
| Flex5                | DTU       | Commercial use |   | Morison equation                         |                                  | DLL              | –                                       |
| Simo/Reflex/ AeroDyn | NTNU      | Indoor         |   | Potential flow theory + Morison equation | FEM                              | DLL              | FEM                                     |
| CHARM3D- FAST        | TAMU      | Indoor         |   |  |                                  |                  |   |

Note: 1- Dynamics of multi-body system, 2-Finite element method, 3-modal analysis method, 4-External dynamic link library, 5-Quasi-static catenary equation, 6-Lumped-mass method.

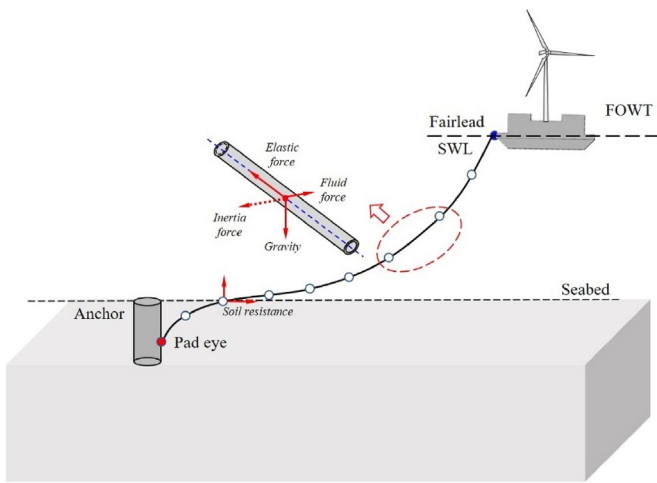


Fig. 8. Forces on the mooring line.

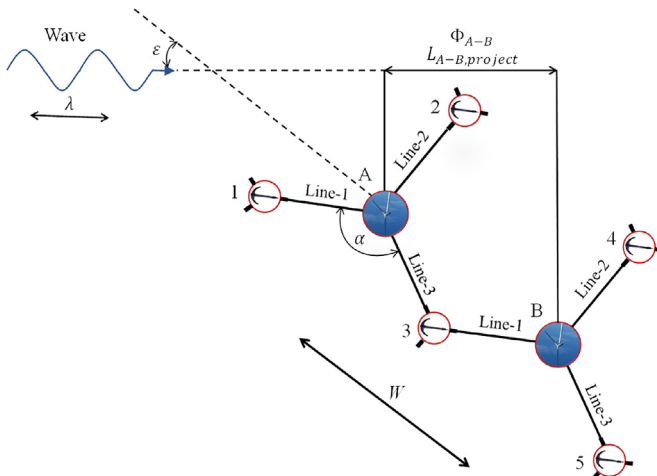


Fig. 9. Simplified calculation method of shared anchor load.

For the shared mooring system, in order to accurately capture the load on the mooring line, it is necessary to consider the accurate representation of the timing of wave loads across the array [50] after defining the coupled motion response of the FOWTs (as stated in section 4.1). It is worth noting that due to the influence of wave propagation speed and the relative positions of the FOWTs, there may be phase differences in the relative motion of different FOWTs, leading to an impact on the tension in the mooring lines. For wind farms with shared anchors, the effect on anchor loads may be even more pronounced. Herduin [79] proposed a simplified estimation method for loads at padeye. As shown in Fig. 9, considering a three-line shared mooring system subjected to regular waves with a wavelength of  $\lambda$ , with the incident wave at an angle  $\varepsilon$  to the line connecting two FOWTs. The distance between FOWT A and B is denoted as  $W$ , and the projection distance parallel to the wave direction between them is  $L_{A-B,project}$ .  $\alpha$  is the angle between the mooring lines of the FOWT (for the three-line shared mooring system,  $\alpha$  is  $120^\circ$ ), and  $\beta$  is the phase angle of the wave from A to B. The load generated by FOWT B at anchor (3, 4, 5) is equal to the load of FOWT A at anchor (1, 2, 3) after considering the time difference. The loads at the three anchors of FOWT A can be taken as the reference mooring load,  $F_{ref}$ , and then transformed into the shared anchor load,  $F_n$ , for the calculation of the tension on the shared anchor using Equation (2).

$$F_n = F_{ref} \sin(2\pi\omega t + \omega_n) \quad (2)$$

where:

$$\omega_n = 2\pi \frac{W \cos(\varepsilon)}{\lambda} \quad (3)$$

In fact, the aforementioned calculation methods are based on several assumptions, such as neglecting wave radiation, second-order wave effects, wake influence, wind-wave coupling, etc. Fontana et al. [80] investigated the spatial coherence of ocean waves in multiline anchor systems for FOWTs with the irregular wave fields, and the results revealed that no consistent trends that differentiated multiline anchor force dynamics generated by spatially independent versus coherent waves. Fontana et al. [80] also pointed out that the analysis is fundamentally linear and based on simple superposition, and the correlation and the maximum loads might be different for non-linear waves. Advanced simulation tools and further research are still needed to account for these factors adequately.

### 5.2. Net force characteristics of shared anchor

For an individual floating structure, the tension in the mooring lines is coupled with the platform motion. The anchor of the mooring system bears the load controlled by the tension at the end of each mooring line. However, for shared mooring systems, the shared anchor simultaneously experiences the tension from multiple mooring lines, and the load on it varies both in time and space. To describe the load characteristics on the shared anchor, Balakrishnan et al. [15] introduced the concept of anchor net force, which is the vector sum of the different tensions acting on the padeye from different mooring lines. Balakrishnan et al. [15]'s research primarily focuses on catenary mooring systems, where they concluded that uplift load does not exist on the anchor. Similarly, Herduin [79] employed a similar approach and expanded the anchor load analysis into three-dimensional space, defining the uplift load angle. As shown in Fig. 10, in the global coordinate system of the anchor, the total force of the load components acting on each shared anchor can be expressed as the summation of the tension components of each mooring line, as represented by Equations (4)–(6):

$$F_{Rx} = \sum_{i=1}^n F_i \cos(\alpha_i) \cdot \cos(\beta_i) \quad (4)$$

$$F_{Ry} = \sum_{i=1}^n F_i \sin(\alpha_i) \cdot \cos(\beta_i) \quad (5)$$

$$F_{Rz} = \sum_{i=1}^n F_i \cdot \sin(\beta_i) \quad (6)$$

where  $n$  denotes the number of mooring lines connected to the shared anchor,  $F_i$  represents the tension in the  $i$ -th mooring line,  $\alpha_i$  represents the horizontal angle between vector  $F_i$  and the origin of the coordinate system, and  $\beta_i$  represents the vertical angle between vector  $F_i$  and the origin of the coordinate system. The net force on the shared anchor  $F_R$ , the horizontal static direction angle of the anchor  $\alpha_R$ , and the uplift net force direction angle of the anchor  $\beta_R$ , can be calculated using Equations (7)–(9). By defining these parameters,  $F_R$ ,  $\alpha_R$ , and  $\beta_R$ , the magnitude and spatial characteristics of the net force load on the shared anchor can be defined accordingly.

$$F_R = \sqrt{F_{Rx}^2 + F_{Ry}^2 + F_{Rz}^2} \quad (7)$$

$$\alpha_R = \tan^{-1} \left( \frac{F_{Ry}}{F_{Rx}} \right) \quad (8)$$

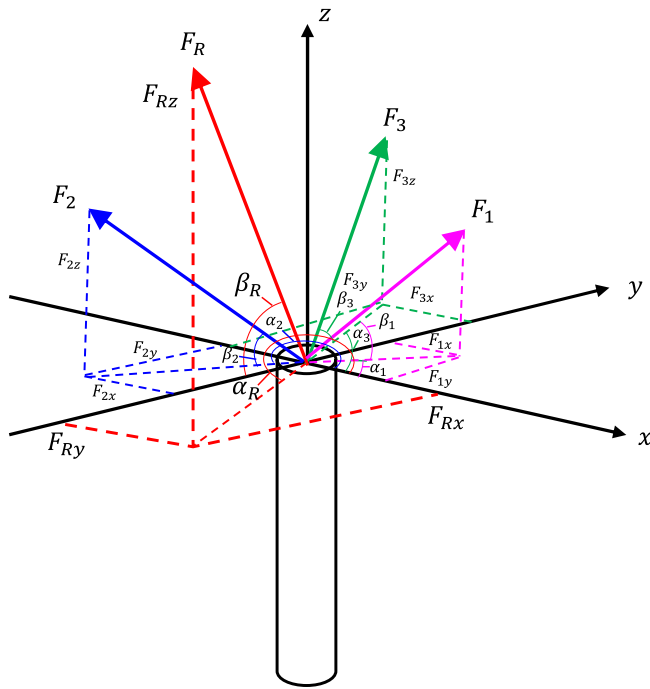
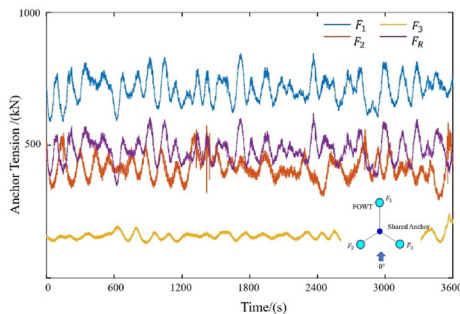
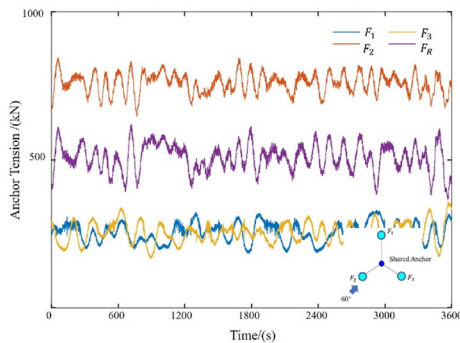


Fig. 10. Net force in the anchor coordinate system.



(a) DLC 1.6 condition 30° wind wave and current incident in the same direction.



(b) DLC 1.6 condition 60° wind wave and current incident in the same direction.

Fig. 11. Net force change of 3-line shared anchor under different load incidence angles (Adapted under the terms of the CC-BY license [15]. Copyright 2020, IOP Publishing).

$$\beta_R = \tan^{-1} \left( \frac{F_{Rz}}{\sqrt{F_{Rx}^2 + F_{Ry}^2}} \right) \quad (9)$$

The scale of a floating offshore wind farm, the type of turbine foundation, variations in water depth, and the layout of the shared mooring system can all impact the net forces on anchors. Generally, due to the

symmetry in conventional shared mooring system layouts such as squares, triangles, hexagons, etc., the net forces acting on the shared anchor in certain directions may cancel each other out. This can be highly advantageous when the entire wind farm is subjected to extreme conditions with wind, wave, and current loads acting in the same direction. It means that the peak loads on the anchors will be reduced, and these peak loads often determine the size of the anchors, directly affecting their cost.

Pillai et al. [61] conducted a series of numerical simulations for a shared mooring system under shallow water conditions (70 m) considering both normal operating and shutdown scenarios. The results showed that using a layout with three-line shared anchoring significantly reduced the peak loads on anchor points when wind, wave, and current loads were aligned along a specific mooring line. Specifically, compared to a single FOWT, the peak load on the most disadvantaged anchor was reduced by up to 67%. In addition, adjusting the mooring radius to reduce the peak load on a single FOWT could achieve a maximum reduction of 56%.

Balakrishnan et al. [15] also arrived at similar conclusions regarding the computation of three-line shared anchor systems. As shown in Fig. 11, under the most disadvantaged environmental conditions, the net force on the anchor is significantly lower than the maximum tension in a single mooring line. Furthermore, at different incident angles, the net force on the anchor experiences varying degrees of reduction. Balakrishnan et al. [15] also compared the magnitude of net anchor tension between SPAR and semi-submersible shared mooring configurations. They found that the SPAR-type FOWT exhibits lower net anchor tension, primarily due to the smaller waterline area of the SPAR-type turbine, which results in reduced hydrodynamic loads from waves.

The presence of shared mooring also alters the directionality of the anchor loads. Balakrishnan et al. [15] calculated that for a semi-submersible wind farm with shared mooring, and found that the load direction experienced a standard deviation of approximately 17° within one computational cycle. This effect may be even more significant when considering asymmetric loading conditions. Additionally, Pillai et al. [61] found that, compared to a single FOWT, the alignment of the anchor loads is no longer always aligned with a single mooring line or a specific environmental load, but represents the integrated effects of environmental conditions and mooring responses for three FOWTs, as shown in Fig. 12. The impact of load directionality should be taken into consideration for factors such as wind turbine power generation efficiency, turbine scale, and mooring anchor design.

## 6. Bearing characteristics of shared anchor

### 6.1. Capacity influence of shared anchor

Due to the connection of multiple mooring lines in shared mooring systems, the load magnitudes acting on each mooring line vary with time. Moreover, the net load magnitude and direction acting on the shared padeye will also exhibit periodic variations over time [81]. These cyclic load variations can decrease the reliability of the entire mooring system. Under the changing loads and directions in the mooring lines, the anchors are prone to evolve into an out-of-plane loading state, where the mooring line tensions deviate from the originally designed plane (Fig. 13). The applied out-of-plane conditions that induce torsional moments potentially lead to an increased level of load on the anchor [82] and significantly impacts the lateral bearing capacity of the anchor. Saviano & Pisano (2017) [83] systematically simulated the influence of installation eccentricity (out-of-plane loading condition) on the suction anchor bearing capacity in clay using a three-dimensional finite element method. Notable results from their study in Fig. 14 revealed a significant reduction in the ultimate lateral capacity of suction anchors due to the out-of-plane loading effect. In particular, when the eccentricity angle reaches 90°, the bearing capacity is reduced by as much as 80%. Additionally, it was observed that the sensitivity of the bearing capacity reduction is highest within the range of 10°–30° of out-of-plane angle.



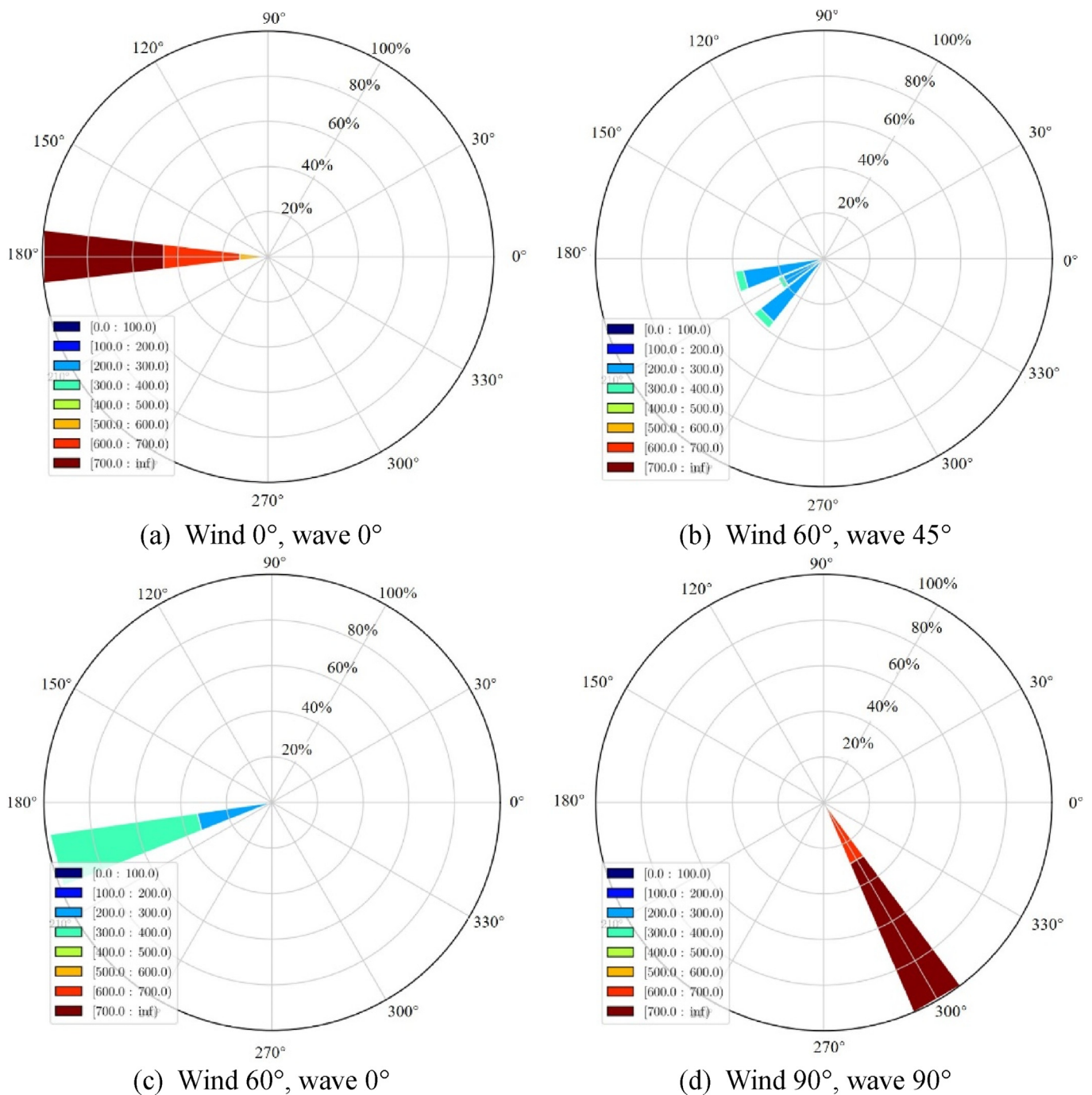


Fig. 12. Load direction changes of shared anchor (Reproduced with permission [61]. Copyright 2022, Elsevier).

This shift in behavior is characterized by a transition from translational failure to torsional failure as the dominant mode of suction anchor failure [84]. Similarly, plate anchors subjected to out-of-plane loading can also have an impact on the bearing capacity [85–87].

During the service life of a FOWT, the shared mooring anchor is subjected to multidirectional loads that undergo millions or even tens of millions of cyclic actions. Previous studies on cyclic loading of individual anchors have got some findings. Firstly, at the scale of soil elements, deep-sea soils are prone to have pore pressure generation and cumulative deformation under cyclic dynamic loads. Their stiffness and strength tend to deteriorate, necessitating the use of more complex constitutive models, such as bounding surface model [88], hypoplasticity model [89], and anisotropic viscoplastic model [90]. Secondly, cyclic shear can lead to

significant displacement weakening and deterioration of the structure-soil interface, resulting in the loss of bearing capacity [91,92]. In terms of the cyclic loading characteristics of suction anchors, model tests have shown that cyclic loading results in a reduction of approximately 10%–20% in the bearing capacity of suction anchors [93–95]. Additionally, Andersen et al. [96] conducted field tests and found that the bearing capacity of suction anchors in clayey soils under cyclic loading decreased to approximately 66%–82% of their static bearing capacity. Singh & Ramaswamy [97] conducted preliminary research on the tension-load behaviour of plate anchors subjected to sustained tension and cyclic loading in saturated soft clay and suggested that the amplitude of cyclic loading should be kept below 30 % of the static anchor capacity to prevent degradation of soil structure and subsequent

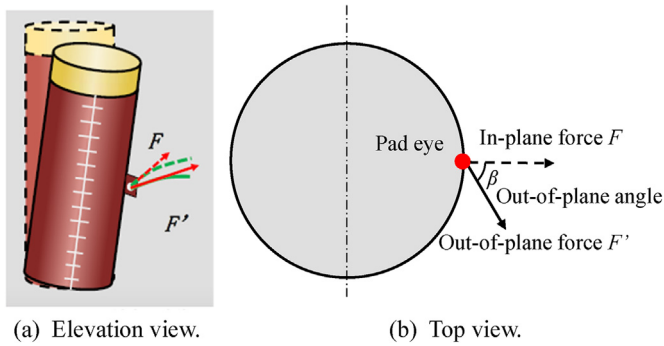


Fig. 13. Out-of-plane loading of suction anchor (Reproduced with permission [84]. Copyright 2023, Elsevier).

loss. In a series of centrifuge tests, Herduin [79] investigated the behavior of short, rigid pile anchors in saturated fine silica sand under multidirectional cyclic loading. The results showed that the strength and direction of cyclic loading significantly influenced the failure mode of the pile anchors. Following multidirectional alternating cyclic loading, the ultimate bearing capacity of the pile anchors was reduced. Compared to single-line anchors, the reduction in bearing capacity reached 56% for two-line shared pile anchors and 86.5% for three-line shared pile anchors. Herduin et al. [79,81] also conducted centrifuge model tests to investigate the behavior of suction anchors under multidirectional cyclic loading. The results similarly indicated a certain degree of loss in the ultimate bearing capacity of suction anchors after multidirectional cyclic

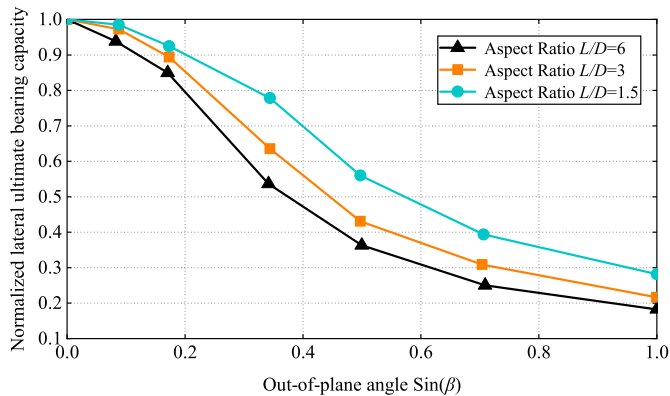
loading. Currently, research on anchors subjected to multidirectional loading is still very limited.

Another potential risk associated with shared anchors is the increased interaction between lines and the seabed. As the number of lines around the anchor increases, their cyclic action can lead to the erosion of shallow soil layers, resulting in two main effects. Firstly, the repeated motion of the lines can cut through the seabed, leading to the formation of trenches in the front of the anchor. Secondly, due to the sediment transport in the shallow seabed, there is more severe overall scouring around the anchor [98]. Seabed trenches have significant inverse influences on the anchor capacity [99–102]. Wang et al. [103] summarized the history cases of seabed trenching near the mooring anchor. Rui et al. [104] and Sun et al. [105] employed finite element or large deformation analysis methods to reproduce the process of suction anchor chains cyclically cutting through the seabed and forming trenches. Sun et al. [106] also proposed plastic upper bound and finite element solutions for the bearing capacity of suction anchors under trench conditions. They found that the undrained ultimate bearing capacity of suction anchors decreases as the trench width increases. A trench with the same width as the suction anchor diameter can result in a maximum reduction of 83% in the bearing capacity, as illustrated in Fig. 15. Similarly, Rui et al. [98] conducted centrifuge model tests using Particle Image Velocimetry (PIV) techniques to investigate shallow loss of suction anchors, and verified that the trench reducing the anchor capacities by changing the anchor failure modes.

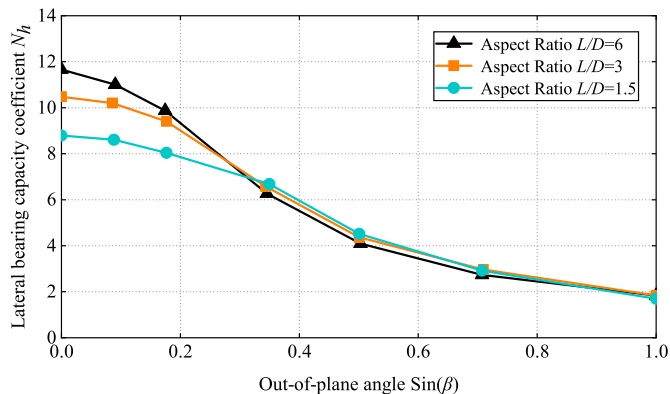
### 6.2. Novel probable shared anchor

The load-bearing characteristics of shared anchors urgently demand innovative, efficient, and reliable designs. Traditional maritime anchor types, commonly employed in offshore engineering, seem to be inapplicable. In consideration of both load-bearing capabilities and economic viability, shared anchors must meet at least two critical requirements: omnidirectional load-bearing and a substantial capacity of anchor. Omnidirectional load-bearing signifies that shared anchor must possess excellent torsional resistance to withstand high-frequency directional changes or out-of-plane loadings. The significant holding capacity of anchor necessitates, on one hand, that these foundations maintain good installation performance and operability, similar to conventional offshore anchors, to meet the requirements of large-scale, cost-effective deployments. On the other hand, they must provide greater load-bearing capacity to mitigate the risk of anchor failure caused by cyclic loading, seabed trench, and other factors.

In light of these requirements, traditional anchors (such as suction anchor, pile anchor plate anchor and gravity anchor) should be under novel design and feasibility assessments. As the most widely utilized anchor type in deep-sea floating structures, suction caisson has undergone extensive practical implementation and analysis regarding its installation and load-bearing capabilities over the past two decades [107–109]. It holds promising potential for development into a fundamental configuration of shared anchor foundations. Fu et al. [82] have proposed a novel form of suction anchor with fins. By adding outer fins, they have extended the traditional suction anchor's 'anchor-soil shear plane' under torsional torque to a 'soil-soil shear plane' (Fig. 16a). This effectively reduces the disturbance caused by the disturbed soil against torsional bearing capacity after anchor installation and increases the shear area of undisturbed native soil. In comparison to traditional suction anchors with the same shear diameter, this design significantly enhances torsional resistance. Lee & Abuney [110] have also introduced a Multi-line Ring Anchor (MRA, Fig. 16b) composed of an embedded ring anchor and multiple wing plates. Numerical simulations indicate that, at the same diameter, its lateral load-bearing capacity can match that of a suction anchor three times its length. Rui et al. [111] has proposed a caisson-plate gravity anchor (CPGA) based on a gravity anchor and caisson-shaped foundation (Fig. 16c). This design effectively addresses the mismatch between anchor installation and load-bearing, significantly increasing its capacity.

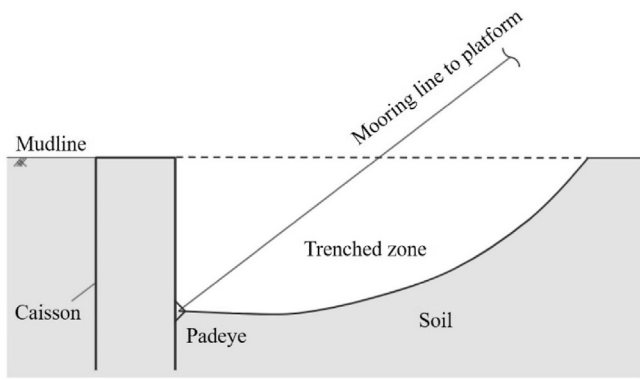


(a) Normalized lateral ultimate bearing capacity.

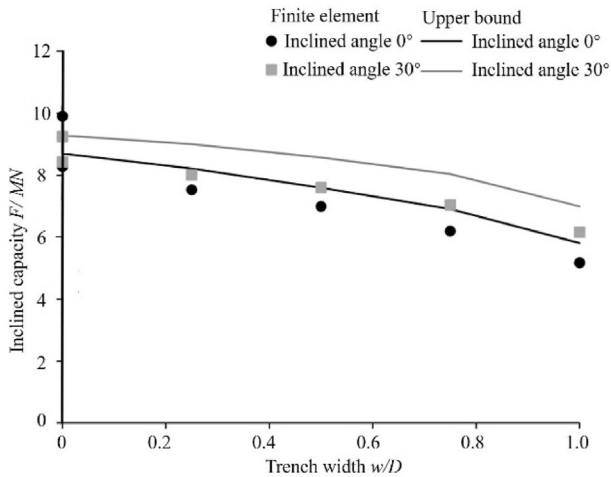


(b) Lateral bearing capacity coefficient.

Fig. 14. Lateral bearing capacity of the suction anchor varied with the out-of-plane angle (Adapted with permission [83]. Copyright 2017, Elsevier).



(a) Trench around suction anchor.

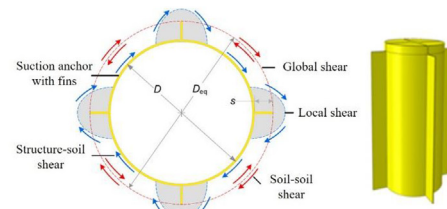


(b) Trench influence on ultimate bearing capacity.

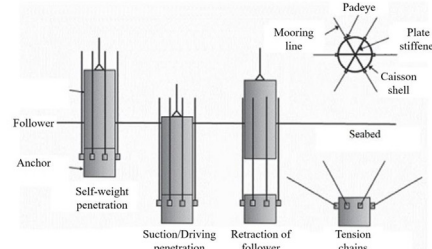
Fig. 15. Trench for suction anchor system (Adapted with permission [106]. Copyright 2022, Emerald Publishing).

Unlike the suction anchor, anchor pile padeyes are usually fixed near the mudline to bear both lateral and vertical loads. The anchor has good adaptability in various types of soil, e.g., clay, sand, and silt [112]. Its installation is typically accomplished through pile driving. Therefore, for floating offshore wind farms in shallow-water regions (e.g., semi-submersible platforms), anchor piles are also considered a suitable choice for shared anchors. Plate anchors with many variants of this type of anchor, e.g., DEA (drag embedded anchor) and SEPLA, are typically triangular or rectangular in shape, with anchor flukes connected through ship movement or chain tension during installation, e.g., drag embedded anchor [113]. Plate anchors have a high capacity and can resist significant vertical uplift forces, making them a cost-effective choice for taut mooring in floating offshore wind farms [114]. The problem of the plate anchor lies in its geometric asymmetry, loading direction sensitivity and positioning inaccuracy, thus the design of this kind of shared anchor needs further improvement. For gravity anchor, their load-bearing capacity primarily relies on their own weight and the friction with the seabed [115,121]. Despite their relatively lower load-bearing efficiency, it is undeniable that their load-bearing performance is the most stable. Therefore, there is also a possibility for them to be developed as shared anchor solutions. Currently, there is limited research on the shared anchor for these configurations.

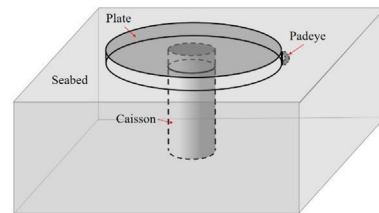
Indeed, besides improvements made to traditional anchor types, there is also great potential for the application of new forms of anchors in shared anchor system. For example, the dynamic penetration anchors (DPA), typically composed of some flukes, which penetrates the soil layers by kinetic energy release [116–118]. Consequently, it possesses the ability of omnidirectional loading. Lieng et al. [119] explored the



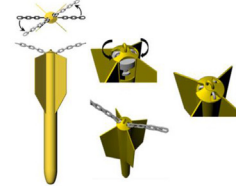
(a) Suction anchor with anti-rotational fins (Adapted with permission. [82] Copyright 2021, Elsevier).



(b) Multiline ring anchor (Reproduced with permission. [110] Copyright 2021, ASCE).



(c) Caisson-plate gravity anchor (reproduced under the terms of the CC-BY license. [111] Copyright 2023, MDPI).



(d) Shared DPA (Reproduced with permission. [118] Copyright 2022, Elsevier).

Fig. 16. Novel probable shared anchors.

feasibility of DPA (Fig. 16d) as shared anchors. The results indicate that an appropriate layout of shared DPA can effectively reduce load amplitude, and the bearing capacity is relatively high, thereby reducing anchor manufacturing and offshore operation costs. But it is noted that DPAs can usually be adopted in temporary moorings, but may not be suitable in permanent moorings due to the difficulty in controlling the installation quality. Another example is screw anchors, which originated from onshore engineering with considerable uplift capacity and can also be considered to be applied in TLP wind farms to resist significant vertical loads [120].

## 7. Conclusions

This paper provides an analysis of the pertinent literature concerning shared mooring systems for floating wind farms, outlines the current state of research in this field, and highlights the existing challenges and issues in their development. The key findings are as follows:

1. The shared mooring design concept presents a fresh solution for clustered or arrayed floating wind farms by reducing the number of anchors and mooring lines, effectively reducing construction costs. It is further revealed that additional comparative studies between various shared mooring layout forms are necessary, and more advanced methods for enhancing the reliability of shared mooring systems need to be developed.

2. The shared mooring approach introduces greater complexity due to the dynamic interaction between FOWTs, aerodynamic wake effects, and hydrodynamic influences. Conventional single FOWT numerical simulation tools are inadequate for simulating the entire wind farm. The motion responses of arrayed FOWTs under equivalent environmental loading conditions are influenced by factors such as mooring layout, turbine size, and wind farm scale.
3. In shared mooring systems, tension loads acting on anchors from multiple mooring lines lead to varying net forces at the padeye both in time and space. Symmetric layouts of shared mooring configurations can reduce peak anchor loads under certain coherent wind, wave, and current conditions. The net force direction for shared moorings depends on a combination of environmental conditions and mooring responses.
4. Under multidirectional loading, shared anchors experience out-of-plane tension from mooring lines, resulting in increased torque loading and potential reduction in load-bearing capacity. Cyclic dynamic loading weakens the anchor-soil interface and the seabed's stiffness and strength, potentially leading to soil loss around shared anchors and reduced bearing capacity.
5. Future innovations should focus on developing more efficient and reliable forms of shared anchors, such as suction anchors with fins, caisson-plate gravity anchors, and others. These designs should be suitable for diverse geological strata, economically viable, and provide reliable bearing capacity to withstand complex loading conditions. Emphasizing omnidirectional load-bearing capabilities is crucial for addressing multidirectional load scenarios and promoting widespread applicability.

#### Declaration of competing interest

The authors declared that they have no conflicts of interest to this work.

We declare that we do not have any commercial or associative interest that represents a conflict of interest in connection with the work submitted.

#### Acknowledgements

The authors gratefully acknowledge the financial supports from the National Natural Science Foundation of China (52101334), the European Commission (HORIZON-MSCA-2022-PF-01, 101108745), the Research Council of Norway (SFI BLUES project, 309281), and the Open Fund from Zhejiang Key Laboratory of Offshore Geotechnics and Material (OGME21003, OGME22001).

#### References

- [1] A.M. Omer, Energy, environment and sustainable development, *Renew. Sustain. Energy Rev.* 12 (2008) 2265–2300, <https://doi.org/10.1016/j.rser.2007.05.001>.
- [2] D. Gielen, F. Boshell, D. Saygin, M.D. Bazilian, N. Wagner, R. Gorini, The role of renewable energy in the global energy transformation, *Energy Strategy Rev.* 24 (2019) 38–50, <https://doi.org/10.1016/j.esr.2019.01.006>.
- [3] Y.L. He, S. Du, S. Shen, Advances in porous volumetric solar receivers and enhancement of volumetric absorption, *Energy Rev.* 2 (5) (2023) 100035, <https://doi.org/10.1016/j.enrev.2023.100035>.
- [4] X. Zha, Z. Guo, L.Z. Wang, S.J. Rui, A simplified model for predicting the accumulated displacement of monopile under horizontal cyclic loadings, *Appl. Ocean Res.* 129 (2022) 103389, <https://doi.org/10.1016/j.apor.2022.103389>.
- [5] L.L. Jiang, D. Xue, Z.X. Wei, Z.X. Chen, M. Mirzayev, Y.P. Chen, S.S. Chen, Coal decarbonization: a state-of-the-art review of enhanced hydrogen production in underground coal gasification, *Energy Rev.* 1 (1) (2022) 100004, <https://doi.org/10.1016/j.enrev.2022.100004>.
- [6] G.S. Li, J.Y. Ji, X.Z. Song, Y. Shi, S. Li, Z.H. Song, F.Q. Xu, Research advances in multi-field coupling model for geothermal reservoir heat extraction, *Energy Rev.* (2022) 100009, <https://doi.org/10.1016/j.enrev.2022.100009>.
- [7] IEA, *Offshore Wind Outlook 2019, World Energy Outlook Special Report*, 2020.
- [8] IRENA, *Floating Foundations: A Game Changer for Offshore Wind Power*, A Supplement to Innovation Outlook, offshore wind, 2016.
- [9] Y.H. Chen, H.Y. Lin, Overview of the development of offshore wind power generation in China, *Sustain. Energy. Techn.* 53 (2022) 102766, <https://doi.org/10.1016/j.seta.2022.102766>.
- [10] GWEC, *Global Wind Report 2018*, Global Wind Energy Council, Brussels, Belgium, 2019.
- [11] WFO, *Global Offshore Wind Report-2022, World Forum Offshore Wind*, 2022.
- [12] W. Musial, P. Spitsen, P. Duffy, P. Beiter, M. Marquis, R. Hammond, M. Shields, *Offshore Wind Market Report: 2022 Edition*, National Renewable Energy Lab, Golden, CO (United States), 2022.
- [13] DNV, *Floating Wind: the Power to Commercialize*, Hovik, Norway, 2020.
- [14] C. Gaudin, C. O'Loughlin, T.M. Duong, M. Herduin, N. Fiumana, S. Draper, H. Wolgamot, L. Zhao, M. Cassidy, New anchoring paradigms for floating renewables, in: *Proceedings of the 12th Europe Wave and Tidal Energy Conference*, UK, 2018.
- [15] K. Balakrishnan, S.R. Arwade, D.J. DeGroot, C. Fontana, M. Landon, C.P. Aubeny, Comparison of multiline anchors for offshore wind turbines with spar and with semisubmersible, *J. Phys.: Conf. Ser.* 1452 (1) (2020) 012032, <https://doi.org/10.1088/1742-6596/1452/1/012032>.
- [16] T. Stehly, P. Beiter, P. Duffy, 2019 Cost of Wind Energy Review, National Renewable Energy Lab, 2020.
- [17] ITIF, *Floating Wind Farms, Climate-Tech to Watch*, 2021.
- [18] European Commission, *Pivotbuoy: an Advanced System for Cost-Effective and Reliable Mooring, Connection, Installation & Operation of Floating Wind*, European Union, 2020.
- [19] EWEA, *Deep Water*, European Wind Energy Association, 2013.
- [20] K.-T. Ma, Y. Luo, T. Kwan, Y.Y. Wu, *Mooring System Engineering for Offshore Structures*, Gulf Professional Publishing, 2019.
- [21] L. Castro-Santos, V. Diaz-Casas, *Floating Offshore Wind Farms*, Spain, 2016.
- [22] J.Y. Chen, M.H. Kim, Review of recent offshore wind turbine research and optimization methodologies in their design, *J. Mar. Sci. Eng.* 10 (1) (2022) 28, <https://doi.org/10.3390/jmse10010028>.
- [23] H. Wang, Catenary mooring, in: W. Cui, S. Fu, Z. Hu (Eds.), *Encyclopedia of Ocean Engineering*, Springer, Singapore, 2020, [https://doi.org/10.1007/978-981-10-6963-5\\_145-1](https://doi.org/10.1007/978-981-10-6963-5_145-1).
- [24] H. Wang, Taut mooring, in: W. Cui, S. Fu, Z. Hu (Eds.), *Encyclopedia of Ocean Engineering*, Springer, Singapore, 2022, [https://doi.org/10.1007/978-981-10-6946-8\\_146](https://doi.org/10.1007/978-981-10-6946-8_146).
- [25] R.J. Smith, C.J. MacFarlane, Statics of a three component mooring line, *Ocean Eng.* 28 (7) (2001) 899–914, [https://doi.org/10.1016/S0029-8018\(00\)00058-5](https://doi.org/10.1016/S0029-8018(00)00058-5).
- [26] F.G. Nielsen, A.U. Bindingbø, Extreme loads in taut mooring lines and mooring line induced damping: an asymptotic approach, *Appl. Ocean Res.* 22 (2) (2000) 103–118, [https://doi.org/10.1016/S0141-1187\(99\)00026-7](https://doi.org/10.1016/S0141-1187(99)00026-7).
- [27] A. Campanile, V. Piscopo, A. Scamardella, Mooring design and selection for floating offshore wind turbines on intermediate and deep water depths, *Ocean Eng.* 148 (2018) 349–360, <https://doi.org/10.1016/j.oceaneng.2017.11.043>.
- [28] B. Wilde, H. Treu, F. Tom, Field testing of suction embedded plate anchors, in: *Paper Presented at the Eleventh International Offshore and Polar Engineering Conference*, Stavanger, Norway, 2001.
- [29] C.C. Han, J. Liu, A review on the entire installation process of dynamically jacked anchors, *Ocean Eng.* 202 (2020) 107173, <https://doi.org/10.1016/j.oceaneng.2020.107173>.
- [30] G. Spagnoli, Some considerations regarding the use of helical piles as foundation for offshore structures, *Soil Mech. Found. Eng.* 50 (3) (2013) 102–110, <https://doi.org/10.1007/s11204-013-9219-7>.
- [31] C. Fontana, S.R. Arwade, D.J. DeGroot, A.T. Myers, M. Landon, C.P. Aubeny, Efficient multiline anchor systems for floating offshore wind turbines, in: *Proceedings of the International Conference on Offshore Mechanics and Arctic Engineering-OMAE*, Busan, South Korea, 2016, pp. 1–7, <https://doi.org/10.1115/OMAE2016-54476>.
- [32] C. Fontana, S. Hallowell, S.R. Arwade, D.J. DeGroot, M.E. Landon, C.P. Aubeny, B. Diaz, A.T. Myers, S. Ozmutlu, Multiline anchor force dynamics in floating offshore wind turbines, *Wind Energy* 21 (11) (2018) 1177–1190, <https://doi.org/10.1002/we.2222>.
- [33] M. Goldschmidt, M. Muskulus, Coupled mooring systems for floating wind farms, *Energy Proc.* 80 (2015) 255–262, <https://doi.org/10.1016/j.egypro.2015.11.429>.
- [34] O. Gözcü, S. Kontos, H. Bredmose, Dynamics of two floating wind turbines with shared anchor and mooring lines, *J. Phys.: Conf. Ser.* 2265 (4) (2022) 042026, <https://doi.org/10.1088/1742-6596/2265/4/042026>.
- [35] Z. Gao, T. Moan, Mooring system analysis of multiple wave energy converters in a farm configuration, in: *Proceedings of the 8th European Wave and Tidal Energy Conference*, Uppsala, Sweden, 2009.
- [36] M. Hall, E. Lozon, S. Housner, S. Srinivas, Design and analysis of a ten-turbine floating wind farm with shared mooring lines, *J. Phys.: Conf. Ser.* 2362 (1) (2022) 012016, <https://doi.org/10.1088/1742-6596/2362/1/012016>.
- [37] P. Connolly, M. Hall, Comparison of pilot-scale floating offshore wind farms with shared moorings, *Ocean Eng.* 171 (2019) 172–180, <https://doi.org/10.1016/j.oceaneng.2018.08.040>.
- [38] S. Wilson, M. Hall, S. Housner, S. Srinivas, Linearized modeling and optimization of shared mooring systems, *Ocean Eng.* 241 (2021), <https://doi.org/10.1016/j.oceaneng.2021.110009>.
- [39] M.C. Devin, B. DuPont, S.T. Hallowell, S.R. Arwade, Optimizing the cost and reliability of shared anchors in an array of floating offshore wind turbines, *Asce-Asme. J. Risk. U. B.* (4) (2021) 7, <https://doi.org/10.1115/1.4051163>.
- [40] S.T. Hallowell, S.R. Arwade, C.M. Fontana, D.J. DeGroot, C.P. Aubeny, B.S. Diaz, A.T. Myers, M.E. Landon, System reliability of floating offshore wind farms with

- multiline anchors, *Ocean Eng.* 160 (2018) 94–104, <https://doi.org/10.1016/j.oceaneng.2018.04.046>.
- [41] S.T. Hallowell, S.R. Arwade, B.D. Diaz, C.P. Aueny, C.M. Fontana, D.J. DeGroot, M.E. Landon, Harmonizing the mooring system reliability of multiline anchor wind farms, *ASCE/ASME J. Risk Reliab.* 7 (4) (2021), <https://doi.org/10.1115/1.4052423>.
- [42] S. Yamamoto, W. Colburn, *Power Generation Assemblies, and Apparatus for Use Therewith*, US8578586B2, 2006.
- [43] R. James, M.C. Ros, *Floating Offshore Wind: Market and Technology Review*, The Carbon Trust, UK, 2015.
- [44] J. He, X. Jin, S.Y. Xie, L. Cao, Y.F. Lin, N. Wang, Multi-body dynamics modeling and TMD optimization based on the improved AFSA for floating wind turbines, *Renew. Energy* 141 (128) (2019), <https://doi.org/10.1016/j.renene.2019.04.005>.
- [45] J. McMorland, M. Collu, D. McMillan, J. Carroll, Operation and maintenance for floating wind turbines: a review, *Renew. Sustain. Energy Rev.* 163 (2022) 112499, <https://doi.org/10.1016/j.rser.2022.112499>.
- [46] B.J. Jonkman, M.L. Buhl, *TurbSim User's Guide*, National Renewable Energy Laboratory, USA, 2006.
- [47] J.M. Jonkman, M.L. Buhl, *FAST User's Guide*, National Renewable Energy Laboratory, USA, 2005.
- [48] A. Robertson, J. Jonkman, F. Vorpahl, M. Guerinel, Offshore Code Comparison Collaboration Continuation within IEA Wind Task 30: Phase II Results Regarding a Floating Semisubmersible Wind System, Preprint, USA, 2014, <https://doi.org/10.1115/OMAE2014-24040>.
- [49] ORCINA, *OrcaFlex Manual, Version 11.3d. Technical Report*, Orcina Limited, 2023.
- [50] E. Lozon, M. Hall, Coupled loads analysis of a novel shared-mooring floating wind farm, *Appl. Energy* 332 (2023) 120513, <https://doi.org/10.1016/j.apenergy.2022.120513>.
- [51] G.D. Liang, Z.Y. Jiang, K. Merz, Mooring analysis of a Dual-Spar floating wind farm with a shared line, *J. Offshore. Mech. Arct.* 143 (6) (2021), <https://doi.org/10.1115/1.4050965>.
- [52] Y.M. Zhang, H.X. Liu, Coupled dynamic analysis on floating wind farms with shared mooring under complex conditions, *Ocean Eng.* 267 (2023) 113323, <https://doi.org/10.1016/j.oceaneng.2022.113323>.
- [53] F. Gonzalez-Longatt, P. Wall, V. Terzija, Wake effect in wind farm performance: steady-state and dynamic behaviour, *Renew. Energy* 39 (2012) 329–338, <https://doi.org/10.1016/j.renene.2011.08.053>.
- [54] M.F. Howland, S.K. Lele, J.O. Dabiri, Wind farm power optimization through wake steering, *P. Natl. Acad. Sci.* 116 (29) (2019) 14495–14500, <https://doi.org/10.1073/pnas.1903680116>.
- [55] N. Cao, Q. Yu, W.S. Wang, L.B. Shi, Research on wake effect model of wind farm, *Acta Energiae Solaris Sin.* 37 (1) (2016) 222–229, <https://doi.org/10.3969/j.issn.0254-0096.2016.01.035>.
- [56] R. Shakoor, M.Y. Hassan, A. Raheem, Y.K. Wu, Wake effect modeling: a review of wind farm layout optimization using Jensen's model, *Renew. Sustain. Energy Rev.* 58 (2016) 1048–1059, <https://doi.org/10.1016/j.rser.2015.12.229>.
- [57] M.F. Qin, W. Shi, W.W. Chai, X. Fu, L. Li, X. Li, Extreme structural response prediction and fatigue damage evaluation for large-scale monopile offshore wind turbines subject to typhoon conditions, *Renew. Energy* 208 (2023) 450–464, <https://doi.org/10.1016/j.renene.2023.03.066>.
- [58] J.G. Njiri, D. Söffker, State-of-the-art in wind turbine control: trends and challenges, *Renew. Sustain. Energy Rev.* 60 (2016) 377–393, <https://doi.org/10.1016/j.rser.2016.01.110>.
- [59] E. Hernandez-Estrada, O. Lastres-Danguillecourt, J. Robles-Ocampo, A.T. López-López, P.Y. Sevilla-Camacho, B.Y. Pérez-Sarriana, J.R. Dorrego-Portela, Considerations for the structural analysis and design of wind turbine towers: a review, *Renew. Sustain. Energy Rev.* (2020) 110447, <https://doi.org/10.1016/j.rser.2020.110447>.
- [60] M. Hall, P. Connolly, Coupled dynamics modelling of a floating wind farm with shared mooring lines, in: *Proceedings of the ASME 2018 37th International Conference on Ocean, Offshore and Arctic Engineering*, Madrid, Spain, ASME, 2018, <https://doi.org/10.1115/OMAE2018-78489.V010T09A087>.
- [61] A.C. Pillai, T.J. Gordelier, P.R. Thies, C. Dormenval, B. Wray, R. Parkinson, L. Ohanning, Anchor loads for shallow water mooring of a 15 MW floating wind turbine-Part I: chain catenary moorings for single and shared anchor scenarios, *Ocean Eng.* 266 (1) (2022) 112619, <https://doi.org/10.1016/j.oceaneng.2022.111816>.
- [62] Q. Din, C. Li, N.T. Yu, W.X. Hao, J. Ji, Numerical and experimental investigation into the dynamic response of a floating wind turbine spar array platform, *J. Mech. Sci. Technol.* 32 (3) (2018) 1106–1116, <https://doi.org/10.1007/s12206-018-0213-x>.
- [63] X.Z. Yue, Q.S. Liu, W.P. Miao, C. Li, Research on dynamic response of semi-submersible floating wind turbine array platform in normal sea state, *J. Eng. Therm. Energy Power* 37 (9) (2022) 152–160, <https://doi.org/10.16146/j.cnki.rndlgc.2022.09.019>, 2022.
- [64] H.S. He, S.J. Li, M.N. Yue, C. Li, Research on dynamic response of floating wind farm platform under wind-wave misalignment, *J. Eng. Therm. Energy Power* 37 (8) (2022) 166–174, <https://doi.org/10.16146/j.cnki.rndlgc.2022.08.021>.
- [65] H. Munir, C.F. Lee, M.C. Ong, Global analysis of floating offshore wind turbines with shared mooring system, *IOP Conf. Ser. Mater. Sci. Eng.* 1201 (1) (2021) 012024, <https://doi.org/10.1088/1757-899X/1201/1/012024>.
- [66] NREL, *OpenFAST Documentation*, NREL Limited, 2023. Technical Report, Version 3.4.1.
- [67] H.O. Berteaux, *Buoy Engineering*, New York, 1976.
- [68] M. Hall, A. Goupee, Validation of a lumped-mass mooring line model with DeepCwind semisubmersible model test data, *Ocean Eng.* 104 (2015) 590–603, <https://doi.org/10.1016/j.oceaneng.2015.05.035>.
- [69] M. Hall, MoorDyn V2: new capabilities in mooring system components and load cases, in: *Proceedings of the ASME 2020 39th International Conference on Ocean, Offshore and Arctic Engineering*, Virtual, Online, ASME, 2020, <https://doi.org/10.1115/OMAE2020-19341.V009T09A078>.
- [70] DNV-RP-E301, *Design and Installation of Fluke Anchors-Recommended Practice*, 2021.
- [71] L.Z. Wang, Z. Guo, F. Yuan, Three-dimensional interaction between anchor chain and seabed, *Appl. Ocean Res.* 32 (2010) 404–413, <https://doi.org/10.1016/j.apor.2010.09.001>.
- [72] L.Z. Wang, Z. Guo, F. Yuan, Quasi-static three-dimensional analysis of suction anchor mooring system, *Ocean Eng.* 37 (2010) 1127–1138, <https://doi.org/10.1016/j.oceaneng.2010.05.002>.
- [73] Z. Guo, L.Z. Wang, F. Yuan, Quasi-static analysis of the multicomponent mooring line for deeply embedded anchors, *J. Offshore. Mech. Arct.* 138 (1) (2016), <https://doi.org/10.1115/1.4031986>.
- [74] L.Z. Xiong, J.M. Yang, W.H. Zhao, Dynamics of a taut mooring line accounting for the embedded anchor chains, *Ocean Eng.* 121 (2016) 403–413, <https://doi.org/10.1016/j.oceaneng.2016.05.011>.
- [75] L.Z. Xiong, D.J. White, S.R. Neubecker, W.H. Zhao, J.M. Yang, Anchor loads in taut moorings: the impact of inverse catenary shakedown, *Appl. Ocean Res.* 67 (2017) 225–235, <https://doi.org/10.1016/j.apor.2017.06.010>.
- [76] S.J. Rui, Z. Guo, L.Z. Wang, H.C. Liu, W.J. Zhou, Numerical investigations on load transfer of mooring line considering chain-seabed dynamic interaction, *Mar. Georesour. Geotechnol.* 39 (12) (2021) 1433–1448, <https://doi.org/10.1080/1064119X.2020.1846646>.
- [77] S.J. Rui, L.Z. Wang, Z. Guo, H. Yang, W.J. Zhou, Axial interaction between anchor chain and sand. Part II: cyclic loading test, *Appl. Ocean Res.* 114 (6) (2021) 102815, <https://doi.org/10.1016/j.apor.2021.102815>.
- [78] S.F. Frankenmolen, D.J. White, C.D. O'loughlin, Chain-soil interaction in carbonate sand, in: *Offshore Technology Conference*, Houston, Texas, USA, 2016, <https://doi.org/10.4043/27102-MS.OTC-27102-MS>.
- [79] M. Herduin, *Multi-directional Loading on Shared Anchors for Offshore Renewable Energy: Definition and Preliminary Investigation into Soil Behaviour and Anchor Performance* [Ph.D. Thesis], The University of Western Australia, Perth, 2019.
- [80] C.M. Fontana, S.T. Hallowell, S.R. Arwade, D.J. DeGroot, M.E. Landon, C.P. Aubeny, Spatial coherence of ocean waves in multiline anchor systems for floating offshore wind turbines, *Ocean Eng.* 184 (2019) 59–73, <https://doi.org/10.1016/j.oceaneng.2019.04.048>.
- [81] M. Herduin, C. Gaudin, M. Cassidy, C. O'Loughlin, J. Hambleton, *Multi-Directional Load Cases on Shared Anchors for Arrays of Floating Structures*, Asian Wave and Tidal Energy Conference, Singapore, Singapore, 2016.
- [82] D.F. Fu, Z.Z. Zhou, Y. Yan, D.L. Pradhan, J. Hennig, A method to predict the torsional resistance of suction caisson with anti-rotation fins in clay, *Mar. Struct.* 75 (2020), <https://doi.org/10.1016/j.marstruc.2020.102866>.
- [83] A. Saviano, F. Pisario, Effects of misalignment on the undrained HV capacity of suction anchors in clay, *Ocean Eng.* 133 (2017) 89–106, <https://doi.org/10.1016/j.oceaneng.2017.01.033>.
- [84] H. Xu, S.J. Rui, K.M. Shen, Z. Guo, Investigations on the mooring safety considering the coupling effect of the mooring line snap tension and anchor out-of-plane loading, *Appl. Ocean Res.* 141 (2023) 103753, <https://doi.org/10.1016/j.apor.2023.103753>.
- [85] R.B. Gilbert, C. Lupulescu, C.H. Lee, J. Miller, M. Kroncke, M. Yang, C.P. Aubeny, J.D. Murff, SS: MODU anchor-analytical and experimental modeling for out-of-plane loading of plate anchors, in: *Offshore Technology Conference*, OnePetro, Houston, Texas, 2009, <https://doi.org/10.4043/20115-MS.OTC-20115-MS>.
- [86] M. Yang, J.D. Murff, C.P. Aubeny, Undrained capacity of plate anchors under general loading, *J. Geotech. Geoenviron.* 136 (10) (2010) 1383–1393, [https://doi.org/10.1061/\(ASCE\)GT.1943-5606.0000343](https://doi.org/10.1061/(ASCE)GT.1943-5606.0000343).
- [87] J.T. Wang, Y.H. Tian, W.L. Liu, L. Wang, Capacity envelope of plate anchors under six degree-of-freedom loads in clay, *Appl. Ocean Res.* 126 (2022) 103267, <https://doi.org/10.1016/j.apor.2022.103267>.
- [88] Z.Y. Yin, Q. Xu, C.S. Chang, Modeling cyclic behavior of clay by micromechanical approach, *J. Eng. Mech.* 139 (9) (2013) 1305–1309, [https://doi.org/10.1061/\(ASCE\)EM.1943-7889.0000516](https://doi.org/10.1061/(ASCE)EM.1943-7889.0000516).
- [89] Y. Hong, B. He, L.Z. Wang, Z. Wang, C.W.W. Ng, D. Mašin, Cyclic lateral response and failure mechanisms of semi-rigid pile in soft clay: centrifuge tests and numerical modelling, *Can. Geotech. J.* 54 (6) (2017), <https://doi.org/10.1139/cgj-2016-0356>.
- [90] L.L. Li, H.B. Dan, L.Z. Wang, Undrained behavior of natural marine clay under cyclic loading, *Ocean Eng.* 38 (16) (2011) 1792–1805, <https://doi.org/10.1016/j.oceaneng.2011.09.004>.
- [91] W.J. Zhou, L.Z. Wang, Z. Guo, J.W. Liu, S.J. Rui, A novel t-z model to predict the pile responses under axial cyclic loadings, *Comput. Geotech.* 112 (2019) 120–134, <https://doi.org/10.1016/j.compgeo.2019.04.027>.
- [92] W.J. Zhou, Z. Guo, L.Z. Wang, J.H. Li, S.J. Rui, Effect of cyclic jacking on sand-pile interface shear behaviour, *Soil Dynam. Earthq. Eng.* 141 (2021) 106479, <https://doi.org/10.1016/j.soildyn.2020.106479>.
- [93] E. Clukey, M.J. Morrison, J. Gariner, The response of suction caissons in normally consolidated clays to cyclic TLP loading conditions, in: *Proceedings of 27th Annual Offshore Technology Conference*, 1995, pp. 909–918, <https://doi.org/10.4043/7796-MS>. Houston, USA.

- [94] M. Iskander, S. El-Gharbawy, R. Olson, Performance of suction caissons in sand and clay, *Can. Geotech. J.* 39 (3) (2002) 576–584, <https://doi.org/10.1139/t02-030>.
- [95] M.F. Randolph, A.R. House, Analysis of Suction Caisson Capacity in Clay, Proceedings of 34th Offshore Technology Conference, Houston, USA, 2002, pp. 151–162, <https://doi.org/10.4043/14236-MS>.
- [96] K.H. Andersen, R. Dyrvik, K. Schrder, Field tests of anchors in clay I: predictions and interpretation, *J. Geotech. Geoenviron. Eng. ASCE* 119 (10) (1993) 1532–1549, [https://doi.org/10.1061/\(ASCE\)0733-9410\(1993\)119:10\(1532\)](https://doi.org/10.1061/(ASCE)0733-9410(1993)119:10(1532)).
- [97] S.P. Singh, S.V. Ramaswamy, Response of plate anchors to sustained-cyclic loading, *Indian Geotech. J.* 32 (2) (2002) 161–172.
- [98] S.J. Rui, Z. Guo, L.Z. Wang, H. Wang, W.J. Zhou, Inclined loading capacity of caisson anchor in South China Sea carbonate sand considering the seabed soil loss, *Ocean Eng.* 260 (2022), <https://doi.org/10.1016/j.oceaneng.2022.111790>.
- [99] F.G. Hernandez-Martinez, M. Saue, K. Schroder, H.P. Jostad, Trenching effects on holding capacity for in-service suction anchors in high plasticity clays, in: SNAME 20th Offshore Symposium, OnePetro, Houston, Texas, USA, 2015.
- [100] E.A. Alderieste, R.H. Romp, S. Kay, A. Lofterød, Assessment of seafloor trench for suction pile moorings: a field case, in: Offshore Technology Conference, OnePetro, Houston, Texas, 2016, <https://doi.org/10.4043/27035-MS>.
- [101] K. Sassi, S. Zehzouh, M. Blanc, L. Thorel, D. Cathie, A. Puech, J.L. Colliat-Dangus, Effect of seabed trenching on the holding capacity of suction anchors in soft deepwater Gulf of Guinea clays, in: Proc. Of Offshore Technology Conference, OTC, Houston, Texas, USA, 2018, <https://doi.org/10.4043/28756-MS>.
- [102] X.W. Feng, S. Gourvenec, D.J. White, Load capacity of caisson anchors exposed to seabed trenching, *Ocean Eng.* 171 (2019), 181–192, <https://doi.org/10.1016/j.oceaneng.2018.09.027>.
- [103] L.Z. Wang, S.J. Rui, Z. Guo, Y.Y. Gao, W.J. Zhou, Z.Y. Liu, Seabed trenching near the mooring anchor: history cases and numerical studies, *Ocean Eng.* 218 (2020) 108233, <https://doi.org/10.1016/j.oceaneng.2020.108233>.
- [104] S.J. Rui, Z.F. Zhou, H.P. Jostad, L.Z. Wang, Z. Guo, Numerical prediction of potential 3-dimensional seabed trench profiles considering complex motions of mooring line, *Appl. Ocean Res.* 139 (2023) 103704, <https://doi.org/10.1016/j.apor.2023.103704>.
- [105] C. Sun, M.F. Bransby, S.R. Neubecker, M.F. Randolph, X.W. Feng, S. Gourvenec, Numerical investigations into development of seabed trenching in semitaught moorings, *J. Geotech. Geoenviron.* 146 (10) (2020), [https://doi.org/10.1061/\(ASCE\)GT.1943-5606.0002347](https://doi.org/10.1061/(ASCE)GT.1943-5606.0002347).
- [106] L.Q. Sun, Y.R. Zhang, X.W. Feng, S. Gourvenec, S. Li, Upper-bound solutions for inclined capacity of suction caissons in a trenched seabed, *Geotechnique* (2022) 1–35, <https://doi.org/10.1680/jgeot.22.00133>.
- [107] K.H. Andersen, J.D. Murff, M.F. Randolph, E.C. Clukey, C.T. Erbrich, H.P. Jostad, C. Supachawarote, Suction anchors for deepwater applications, in: n/a, in: M.J. Cassidy, S. Gourvenec (Eds.), Proceedings of the International Symposium on Frontiers in Offshore Geotechnics, CRC Press, Perth, Australia, 2005, pp. 3–30.
- [108] M.F. Randolph, S. Gourvenec, Offshore Geotechnical Engineering, CRC Press, London, 2011.
- [109] DNV-RP-E303, Geotechnical Design and Installation of Suction Anchors in Clay, 2021.
- [110] J. Lee, C.P. Aubeny, Lateral undrained capacity of a multiline ring anchor in clay, *Int. J. GeoMech.* 5 (2021) 21, [https://doi.org/10.1061/\(ASCE\)GM.1943-5622.000199](https://doi.org/10.1061/(ASCE)GM.1943-5622.000199).
- [111] S.J. Rui, H. Xu, L. Teng, C. Xi, X.Y. Sun, H.J. Zhang, K.M. Shen, A framework for mooring and anchor design in sand considering seabed trenches based on floater hydrodynamics, *Sustainability* 15 (12) (2023) 9403, <https://doi.org/10.3390/su15129403>.
- [112] R.J. Jardine, F.C. Chow, R.F. Overy, J.R. Standing, ICP Design Methods for Driven Piles in Sands and Clays, Thomas Telford, London, 2005.
- [113] L.Z. Wang, K.M. Shen, L.L. Li, Z. Guo, Integrated analysis of drag embedment anchor installation, *Ocean Eng.* 88 (5) (2014) 149–163, <https://doi.org/10.1016/j.oceaneng.2014.06.028>.
- [114] DNV-RP-E302, Design and Installation of Plate Anchors in Clay, 2021.
- [115] S.J. Rui, L.Z. Wang, Z. Guo, X.M. Cheng, B. Wu, Monotonic behavior of interface shear between carbonate sands and steel, *Acta Geotech.* 16 (6) (2021) 167–187, <https://doi.org/10.1007/s11440-020-00987-9>.
- [116] H.J. Zhang, Z. Guo, L.Z. Wang, S.J. Rui, R.H. Zhu, X.K. Zhang, Numerical investigations on the installation of dynamically installed anchors with attached mooring line, *Appl. Ocean Res.* 139 (2023) 103716, <https://doi.org/10.1016/j.apor.2023.103716>.
- [117] S.J. Rui, H.J. Zhang, H. Xu, X. Zha, M.T. Xu, K.M. Shen, Seabed structures and foundations related to deep-sea resource development: a review based on design and research, *Deep Undergr. Sci. Eng.* 2 (2023) 1–18, <https://doi.org/10.1002/dug2.12042>.
- [118] Z. Ma, Y. Zheng, L. He, J. Li, Effect of joints on microwave fracturing of the Bukit Timah granite using an open-ended antenna, *Deep Undergr. Sci. Eng.* 1 (2) (2022) 138–147, <https://doi.org/10.1002/dug2.12024>.
- [119] J.T. Lieng, H. Sturm, K.K. Hasselø, Dynamically installed anchors for floating offshore wind turbines, *Ocean Eng.* 266 (2022) 112789, <https://doi.org/10.1016/j.oceaneng.2022.112789>.
- [120] B. Cerfontaine, J. Knappett, M.J. Brown, C. Davidson, Y. Sharif, Optimised design of screw anchors in tension in sand for renewable energy applications, *Ocean Eng.* 217 (2020) 108010, <https://doi.org/10.1016/j.oceaneng.2020.108010>.
- [121] S.J. Rui, L.Z. Wang, Z. Guo, W.J. Zhou, Y.J. Li, Cyclic behavior of interface shear between carbonate sands and steel, *Acta Geotechnica* 16 (2021) 189–209, <https://doi.org/10.1007/s11440-020-01002-x>.